INTERNATIONAL JOURNAL OF ADAPTIVE CONTROL AND SIGNAL PROCESSING
Int. J. Adapt. Control Signal Process. 2014; **28**:444–463
Published online 9 November 2012 in Wiley Online Library (wileyonlinelibrary.com). DOI: 10.1002/acs.2367

Offset-free multistep nonlinear model predictive control under plant–model mismatch

Xuemin Tian [1], Ping Wang [1], Dexian Huang [2] and Sheng Chen [3,4,*,†]

[1] *College of Information and Control Engineering, China University of Petroleum (East China), Dongying, Shandong 257061, China*
[2] *Department of Automation, Tsinghua University, Beijing 10084, China*
[3] *Electronics and Computer Science, Faculty of Physical and Applied Sciences, University of Southampton, Southampton SO17 1BJ, UK*
[4] *Faculty of Engineering, King Abdulaziz University, Jeddah 21589, Saudi Arabia*

SUMMARY

A multistep nonlinear model predictive control (MPC) framework is developed to achieve steady-state offset-free control in the presence of plant–model mismatch. Our formulation explicitly accounts for the effect of plant–model mismatch by involving the output feedback error, which is expressed as the difference between the measured process output and the predicted model output at the previous sampling instance, in the multistep model recursive prediction. The proposed scheme is capable of improving the performance of nonlinear MPC, because the plant–model mismatch is effectively compensated through the recursive prediction propagation. We prove that this formulation is able to remove the steady-state error to achieve offset-free control. The proposed nonlinear MPC framework is applied to a highly nonlinear two-input two-output continuous stirred tank reactor, in comparison with other MPC implementations. The results obtained demonstrate that the proposed technique outperforms some existing popular MPC schemes and can realise offset-free control even under significant plant–model mismatch and unmeasured disturbances. Copyright © 2012 John Wiley & Sons, Ltd.

Received 10 October 2011; Revised 10 October 2012; Accepted 19 October 2012

KEY WORDS: nonlinear model predictive control; offset free; multistep model prediction; plant–model mismatch

1. INTRODUCTION

Model predictive control (MPC), which is referred to as a class of control algorithms utilising an explicit process model to predict the future response of a plant, has become popular in process industries [1, 2]. In an MPC scheme, a dynamic model is first developed to predict the future process outputs in the prediction horizon, based on which future control actions are then computed to minimise a prespecified cost function. Therefore, the effectiveness of MPC relies heavily on the availability of a reasonably accurate process model [3]. MPC algorithms based on linear models are unable to control effectively the nonlinear systems operating over a wide range of operational conditions and with distinctly different input–output behaviours. Analysis and synthesis of MPC schemes based on nonlinear models directly has been an important area of research over the past decade [4]. The introduction of nonlinear models in MPC formulations may solve some problems concerning the nonlinear nature of processes, but the mismatch between the model and the actual

*Correspondence to: Sheng Chen, Electronics and Computer Science, Faculty of Physical and Applied Sciences, University of Southampton, Southampton SO17 1BJ, UK.

†E-mail: sqc@ecs.soton.ac.uk

process inevitably exists [5, 6]. Furthermore, unmeasured disturbances will widen the gap between the model and the process which in turn may lead to degradation in MPC performance. Although the inherent feedback mechanism can tolerate the plant–model mismatch to a certain extent, conventional MPC formulations cannot guarantee steady-state offset-free control [6–8]. The steady-state offset error refers to a persistent discrepancy between the desired set-point value and the actual output of the process.

To combat the offset problem caused by plant–model mismatch or unmeasured disturbances, various methods have been proposed [9–18]. The most widely used scheme in industrial MPC implementations [1, 3] generates the output targets by shifting the set points to compensate for plant–model mismatch, assuming that the plant–model mismatch is due to step disturbances in the output and the disturbance remains constant throughout the prediction horizon. As this correcting scheme is originally employed in the dynamic matrix control (DMC) algorithm, it is known as the DMC-like correcting scheme for offset-free control [1, 3]. This method has been shown to eliminate steady-state offset in some cases, but it cannot effectively deal with the disturbances in the inputs. On the basis of the steady-state target optimisation, the works [12–14] augment the plant model with a disturbance model and use the combined model to estimate the size of the disturbance. Although a number of studies [4–8] have shown that different disturbance models will lead to the different levels of closed-loop performance in the presence of different unmeasured disturbances or plant–model mismatch, there exist insufficient practical guidelines for designing nonlinear MPC (NMPC) disturbance model [6, 10]. Using state observers in MPC formulation is another common method for removing steady-state offset. For nonlinear process, Huang *et al.* [17] have proposed an offset-free NMPC formulation that integrates both the state and output disturbances from the extended Kalman filter. Recently, the authors of [18] have used the moving horizon estimation instead of extended Kalman filter to deal with state inequality constraints. However, the accuracy of a state estimator also heavily depends on the accuracy of the prediction model and, moreover, the dynamics of the state estimator is often required to be much faster than the dynamics of the state feedback control law, which means that the error signal between the observer and the actual system should converge to zero at a much faster rate than the convergence rate of the system state. Sometimes, a state observer may still be used even when the state itself is measurable, which will inevitably impose some additional computational complexity in MPC implementation.

The plant–model mismatch problem is particularly critical to black-box model-based MPC algorithms, because a black-box model may be unduly extrapolated into the regions of the state space where identification data were scarce or nonexistent [19]. The emphasis of black-box model-based NMPC algorithms has mainly focused on developing the models with good long-range prediction capability and/or finding the efficient methodologies to reduce the on-line computational burden. However, there exist relatively few publications in the area of black-box model-based NMPC that can effectively deal with the issue of plant–model mismatch. Psichogis and Ungar [20] have utilised a feed-forward neural network (FNN) model in the conventional MPC scheme, where steady-state offsets are observed to exist during set-point tracking. The corrections to the output are then made using a constant disturbance estimate to obtain offset-free tracking. The authors of [21] have studied the effect of two common types of neural network, FNN and external recurrent network, on the performance of multistep NMPC, and their results show that the steady-state offset of the NMPC algorithm using FNN models will always occur when the prediction horizon is longer than the control horizon. Lu and Tsai [22] have presented a design methodology for the generalised predictive control via recurrent fuzzy neural network. The generalised predictive control law with integral action is derived on the basis of the minimisation of a modified predictive performance criterion, and the simulations and experiments have shown that this method is capable of controlling the processes with satisfactory performance under set point and load changes. Zhang *et al.* [23] have developed an alternative offset-free output feedback NMPC approach based on fuzzy models and an integrating disturbance model, where an augmented piecewise observer is used to estimate the system states and lumped disturbances. However, all the aforementioned studies rely heavily on the special structures of predictive model and are difficult to extend to other forms of model.

Our motivation is to provide an efficient design methodology to achieve the steady-state offset-free control in multistep NMPC. We note the fact that, for multistep prediction, the predictive model is recursively used and the accuracy of the previous-step predictions directly affects the quality of the next-step prediction. Therefore, we propose a scheme in which the previous predictions are firstly corrected by the output feedback error and then used as the input of the predictive model to provide further prediction. The incorporation of the feedback error into multistep prediction will improve the MPC performance, because the information about plant–model mismatch and/or unmeasured disturbances are directly and effectively included in the MPC multistep prediction formulation. Specifically, the plant–model mismatch and/or unmeasured disturbances, manifested as the previous output feedback error, are successively corrected or compensated in the multistep recursive prediction propagation. The advantages of this new formulation are that the steady-state offset can always be eliminated once the process reaches a steady state without imposing additional computational complexity and the only measurement required is the process output. In addition, the proposed offset-free MPC strategy is very practical, as it only needs slightly change to the traditional MPC formulation, and the resulting offset-free NMPC algorithm can adopt a variety of prediction model forms. We use the highly nonlinear continuously stirred tank reactor (CSTR) process [24–30], as a benchmark to compare the performance of the proposed multistep NMPC strategy with the most widely adopted multistep NMPC scheme based on DMC-like correcting. Our results obtained demonstrate that the proposed method, which offers better performance than this existing scheme, is capable of achieving the offset-free control in the presence of significant model mismatch and unmeasured disturbances.

Before presenting the details of our new scheme, we highlight our novel contributions and emphasise the differences of our method with typical related works. Various techniques for achieving steady-state offset-free control may be divided into two classes.

(1) A classical approach to avoid steady-state offset is by introducing an integrator in the control loop, similar to the case of PI control. For nonlinear systems, this can be realised by introducing the control variable increments and augmenting or expanding the system state variables, for example, [9, 31, 32]. However, this will inevitably increase the dimension of the controlled system and therefore significantly increases the computational complexity of NMPC on-line optimisation. Furthermore, to ensure the closed-loop stability of the augmented system, it is generally required to compute and set the steady-state values of the input and state variables corresponding to the desired equilibrium (see Assumption in Lemma 2 of [9]). This is very difficult if not impossible to achieve in the presence of plant–model mismatch. This seriously restricts the application of this approach to practical industrial processes. Moreover, the integral action, which is introduced in front of the plant, does not generally guarantee that the controller can achieve the steady-state zero-error regulation if a state-feedback control law is used [32], and therefore, an observer needs to be introduced even if the system states are available.

    By contrast, our proposed scheme does not require the computation of the steady-state values of the input and state variables at the desired equilibrium, and the steady-state offset-free control is achieved entirely by output feedback without the need of relying on state observer. Moreover, our scheme is computationally more attractive than the schemes of [9, 31, 32].

(2) The other approach to avoid steady-state offset in the presence of plant–model mismatch and external disturbance is to model the plant–model mismatch or external disturbance and then use the output of this model to compensate the effects of plant–model mismatch or external disturbance to the controller. Examples of this second class include the DMC-like correcting scheme widely adopted in practice, the work [33], the approach of [18] and our proposed scheme. The scheme [33] is based on an adaptive disturbance estimation method with time-varying forgetting, where the disturbance is modelled as an integrated moving average process with one lag and is estimated using an adaptive technique that discounts old measurements. However, a linear model, namely, an integrated moving average process with one lag, does not provide an adequate representation for the plant–model mismatch or disturbance in practice, especially when the plant is nonlinear. By contrast, our proposed method is applicable to the generic case of nonlinear plant–model mismatch or disturbance. We use the

DOI: 10.1002/acs

plant–model mismatch or the error between the plant output and model prediction to compensate the controller. However, unlike the conventional multistep prediction method that first makes predictions and then corrects them, our method first corrects the previous predictions by the output feedback error and then uses the compensated previous predictions as the inputs of the predictive model to provide further prediction. This approach is very simple to implement, and our analysis and simulation results confirm that it is very effective in achieving steady-state offset control.

The moving horizon estimation-based formulation [18] requires both nonlinear state-space equation model and nonlinear output measurement equation model of the underlying nonlinear process. If the state-space equation is known and is substituted into the output/measurement equation, then the formulation in [18] appears to 'reduced' to our formulation. In reality, however, our input–output model-based formulation has significant practical and implementation advantages. Firstly, our input–output-based nonlinear auto-regressive exogenous (NARX) model can be easily obtained with black-box data-drive identification procedures. By contrast, it is very difficult to obtain a state-space nonlinear model with data-drive identification algorithms. It is also very difficult to recast an identified nonlinear input–output model into a state-space one. Secondly, our scheme of achieving zero offset is computationally much simpler than the scheme of [18]. Let us assume that the state-space model can be obtained. Every step of the on-line optimisation for the NMPC scheme of [18] requires to solve the on-line state observer estimation optimisation, and it must wait for this state observer to converge. This inevitably increases on-line optimisation complexity dramatically, which may even make the scheme of [18] impractical, particularly if the state observer convergence horizon is long.

Our proposed approach does have a limitation. If the plant has some physical variables that are unmeasurable but are required to meet strict constraints, then it is difficult for our method to guarantee that these unmeasured 'state variables' meet their constraints because these variables are not presented in the input–output model. In this case, an observer-based state estimation approach may have to be used.

The structure of this contribution is organised as follows. Multistep NMPC formulation is introduced in Section 2, whereas Section 3 discusses the most widely used DMC-like correcting scheme to deal with the offset problem and presents our new multistep NMPC scheme for offset-free control. The simulation results are shown in Section 4 to demonstrate the effectiveness of the proposed methodology, and our conclusions are given in Section 5.

2. MULTISTEP NONLINEAR MODEL PREDICTIVE CONTROL FORMULATION

Consider the controlled nonlinear process described by the following discrete-time nonlinear equation

$$\mathbf{y}(k) = \mathbf{f}\left(\mathbf{y}(k-1), \cdots, \mathbf{y}(k-n_y), \mathbf{u}(k-1), \cdots, \mathbf{u}(k-n_u)\right), \tag{1}$$

where k denotes the sampling instant, $\mathbf{f}(\bullet)$ represents the unknown m_y-dimensional nonlinear vector mapping of the controlled process, $\mathbf{y}(k) \in \mathbb{R}^{m_y}$ and $\mathbf{u}(k) \in \mathbb{R}^{m_u}$ are the process's m_y-dimensional output and m_u-dimensional input variables, respectively, whereas n_y and n_u refer to the maximum lags in the process output and input, respectively.

2.1. *Multistep model prediction*

Nonlinear MPC involves using a nonlinear model to predict future process behaviour so that the controlled variables can be manipulated in order for the controlled process to meet the desired target. The performance of MPC relies crucially on the quality of the process model, which is used to generate these predictions [6]. A number of researchers have developed nonlinear models using a variety of technologies [34], including first-principle and black-box approaches. A first-principle model can be valid globally and can predict the system dynamics over the entire operating range. However, development of a reliable first-principle model is a difficult and time-consuming task.

DOI: 10.1002/acs

On the other hand, the nonlinear black-box models have certain advantages over the first-principle models in terms of development time and modelling efforts. We adopt a general NARX model structure [35, 36] to model the process described in (1)

$$\mathbf{y}_m(k) = \mathbf{f}_m\left(\mathbf{y}(k-1), \cdots, \mathbf{y}(k-\hat{n}_y), \mathbf{u}(k-1), \cdots, \mathbf{u}(k-\hat{n}_u)\right), \tag{2}$$

where $\mathbf{f}_m(\bullet)$ denotes the constructed m_y-dimensional model vector mapping, $\mathbf{y}_m(k) \in \mathbb{R}^{m_y}$ is the model output, and $\hat{n}_y$ and $\hat{n}_u$ denote the maximum lags of the output and input in the model, respectively. Note that $\hat{n}_y$ and $\hat{n}_u$ are not necessarily equal to n_y and n_u. The model structure (2) is widely adopted in data-driven nonlinear modelling and control applications [36, 37]. Many existing NMPC algorithms, which employ FNN [38] or support vector regression (SVR) [39] based nonlinear prediction models, also adopt this model structure to model the process.

Accurate multistep prediction is essential if MPC is to be successfully executed. However, the model (2) is identified in the form of the one-step-ahead prediction for the process output. To realise multistep-ahead prediction, the past process output samples in the model input vector are gradually replaced by their predicted values. That is, by feeding back the model outputs, the one-step-ahead predictive model can be recursively cascaded to itself to generate the future predictions for the process output [40]. This procedure is repeated until the predicted output trajectory over the whole prediction horizon is obtained. More specifically, by defining $\mathbf{y}_m(k+i|k)$ as the prediction for the process output $\mathbf{y}(k+i)$ based on the available measurements at the sampling instant k, then this multistep model prediction procedure is described as follows:

$$\begin{aligned} \mathbf{y}_m(k+i-j|k) &= \mathbf{y}(k+i-j),\ \forall j \geqslant i, \\ \mathbf{y}_m(k+i|k) &= \mathbf{f}_m\big(\mathbf{y}_m(k+i-1|k), \cdots, \mathbf{y}_m(k+i-\hat{n}_y|k), \\ &\qquad \mathbf{u}(k+i-1), \cdots, \mathbf{u}(k+i-\hat{n}_u)\big),\ 1 \leqslant i \leqslant P, \end{aligned} \tag{3}$$

where P represents the prediction horizon.

2.2. Nonlinear model predictive control formulation

On the basis of the multistep prediction (3), the MPC design problem at the sampling instant k is defined as the constrained optimisation problem whereby the future manipulated input moves are determined by minimising the objective function:

$$\begin{aligned} \min_{\Delta\mathbf{u}(k|k), \cdots, \Delta\mathbf{u}(k+M-1|k)} & \sum_{i=1}^{P} \left(\mathbf{y}_{\mathrm{sp}} - \mathbf{y}_{\mathrm{p}}(k+i|k)\right)^{\mathrm{T}} \mathbf{Q} \left(\mathbf{y}_{\mathrm{sp}} - \mathbf{y}_{\mathrm{p}}(k+i|k)\right) \\ & + \sum_{j=0}^{M-1} (\Delta\mathbf{u}(k+j|k))^{\mathrm{T}} \mathbf{R} \Delta\mathbf{u}(k+j|k), \end{aligned} \tag{4}$$

subject to the following constraints:

$$\begin{aligned} \mathbf{y}_{\mathrm{p}}(k+i|k) &= \mathbf{y}_m(k+i|k), \quad 1 \leqslant i \leqslant P, \\ \mathbf{y}_{\min} \leqslant \mathbf{y}_{\mathrm{p}}(k+i|k) &\leqslant \mathbf{y}_{\max}, \quad 1 \leqslant i \leqslant P, \end{aligned} \tag{5}$$

$$\begin{aligned} \mathbf{u}_{\min} \leqslant \mathbf{u}(k+j|k) &\leqslant \mathbf{u}_{\max}, \quad 0 \leqslant j \leqslant M-1, \\ \Delta\mathbf{u}_{\min} \leqslant \Delta\mathbf{u}(k+j|k) &\leqslant \Delta\mathbf{u}_{\max}, \quad 0 \leqslant j \leqslant M-1, \end{aligned} \tag{6}$$

where $\mathbf{y}_{\mathrm{sp}} \in \mathbb{R}^{m_y}$ is the set point of the controlled variable, $\mathbf{Q}$ is the $m_y \times m_y$ positive-definite output error weighting matrix, M denotes the control horizon, $\mathbf{R}$ is the $m_u \times m_u$ positive-definite input move weighting matrix and $\Delta\mathbf{u}(k+j|k) = \mathbf{u}(k+j|k) - \mathbf{u}(k+j-1|k)$ is the future control increment, whereas $\mathbf{u}(k+j|k)$ denotes the control action at the future sampling instant $k+j$ based on the available measurements at k. It is assumed that $\Delta\mathbf{u}(k+j|k) = \mathbf{0}$ for $j \geqslant M$. The vector inequality in (5) and (6) is defined as the element-wise inequality operation.

DOI: 10.1002/acs

Given the multistep prediction model (3), the two weighting matrices $\mathbf{Q}$ and $\mathbf{R}$ and the constraints on the output, control input and control input move, $\mathbf{y}_{\min}$, $\mathbf{y}_{\max}$, $\mathbf{u}_{\min}$, $\mathbf{u}_{\max}$, $\Delta\mathbf{u}_{\min}$ and $\Delta\mathbf{u}_{\max}$, the resulting constrained nonlinear optimisation problem can be solved using standard nonlinear programming techniques. The controller is implemented in a moving horizon framework. Thus, after solving the optimisation problem, only the first control action, denoted as $\mathbf{u}_{\mathrm{opt}}(k|k)$, is implemented on the plant, and the optimisation problem is reformulated at the next sampling instant $k+1$, based on the updated information from the process. The weighting parameters, $\mathbf{Q}$ and $\mathbf{R}$, and the prediction and control horizons, P and M, can be tuned to achieve the desired closed-loop performance, and different tuning criteria can be found in [1].

Under the assumption that the actual system is identical to the model used for prediction, the asymptotic stability of the NMPC controller may be guaranteed with several techniques (see, e.g. [41–43]). In [44], the robustness properties of the NMPC have been investigated with respect to the process gain and additive perturbations. Assuming Lipschitz continuity of the MPC law, the authors of [45] have investigated the perturbed asymptotic stability of the NMPC in the face of decaying perturbations. In [46], a robust feasible NMPC is obtained for a given bound on the admissible uncertainties. Some results have been also proposed for the solution of the tracking problem with guaranteed stability. In [47], for example, the tracking of constant signals is solved for the system described by an input/output NARX model. Generally, some additional stability constraints should be introduced to ensure the stability of the closed-loop system [9, 31, 32]. However, it is noted that the introduction of additional stability constraints would always result in some conservatism in the design and performance of MPC controller, particularly in most real-world applications. Comprehensive review on stability and robustness of NMPC can be found in [48, 49]. In industrial applications of NMPC, however, the stability of the closed-loop system and the performance of the control system are traditionally achieved by adjusting the prediction and control horizons and the weighting matrices $\mathbf{Q}$ and $\mathbf{R}$ via trial and error, which is also the approach we adopted in this work.

3. OFFSET-FREE NONLINEAR MODEL PREDICTIVE CONTROL

In the standard NMPC formulation discussed in Section 2, control feedback is manifested as follows: the manipulated input computed for the present time step is implemented on the plant, then the prediction horizon is moved forward one step and the problem is resolved using the new process measurements. Although this formulation exhibits certain robustness to disturbances [7, 8], the robustness of this NMPC does not mean that it can achieve steady-state offset-free control in practical situations. Therefore, some form of correcting mechanism is required to improve the closed-loop performance in the presence of plant–model mismatch and/or unmeasured disturbances.

3.1. Dynamic matrix control-like correcting scheme for offset-free control

As discussed in the Introduction section, most current NMPC implementations use a constant bias calculated on the basis of the current measurement to correct the model–process mismatch [1, 3]. The bias is generated by comparing the measured process output $\mathbf{y}(k)$ and the predicted process output $\mathbf{y}_m(k)$ at the current sampling instant k as

$$\mathbf{e}(k) = \mathbf{y}(k) - \mathbf{y}_m(k), \tag{7}$$

where $\mathbf{y}_m(k) = \mathbf{y}_m(k|k)$ is the model prediction generated by (3) at k. This bias is assumed to remain constant in the future and is utilised to correct the prediction model (3) as

$$\mathbf{y}_{\mathrm{p}}(k+i|k) = \mathbf{y}_m(k+i|k) + \mathbf{e}(k), \; 1 \leqslant i \leqslant P. \tag{8}$$

In other words, the NMPC algorithm based on the DMC-like correcting scheme is obtained by simply replacing the constraints (5) in the standard NMPC algorithm with

$$\begin{aligned} \mathbf{y}_{\mathrm{p}}(k+i|k) = \mathbf{y}_m(k+i|k) + \mathbf{e}(k), \quad 1 \leqslant i \leqslant P, \\ \mathbf{y}_{\min} \leqslant \mathbf{y}_{\mathrm{p}}(k+i|k) \leqslant \mathbf{y}_{\max}, \quad 1 \leqslant i \leqslant P. \end{aligned} \tag{9}$$

DOI: 10.1002/acs

This approach is widely used in industrial MPC implementations, as it can eliminate steady-state offset in some cases [1, 3]. However, we point out that it cannot eliminate the steady-state offset in general. This issue will be further discussed later. In the simulation study, it will also be confirmed that this DMC-like correcting scheme cannot guarantee offset-free control in the presence of strong plant–model mismatch and/or unmeasured disturbances.

3.2. *Proposed correcting scheme for offset-free control*

Because the aforementioned DMC-like correcting scheme cannot guarantee steady-state offset-free behaviour in general, alternative correcting scheme is required to eliminate steady-state offset under the generic plant–model mismatch and unmeasured disturbances. Unlike the DMC-like correcting scheme that only uses the constant bias or output feedback error (7) to correct the multistep predictions generated by the multistep predictive model (3), we propose a correcting scheme in which the previous model predictions are first corrected by the output feedback error term (7) and then used as the input of the multistep predictive model to provide the further prediction. Specifically, given the output feedback error (7), the multistep prediction procedure of (3) is modified as

$$\begin{aligned}\tilde{\mathbf{y}}_m(k+i-j|k) &= \mathbf{y}(k+i-j),\ \forall j \geqslant i,\\ \tilde{\mathbf{y}}_m(k+i|k) &= \mathbf{f}_m\left(\tilde{\mathbf{y}}_m(k+i-1|k), \cdots, \tilde{\mathbf{y}}_m(k+i-\hat{n}_y|k),\right.\\ &\qquad \left.\mathbf{u}(k+i-1), \cdots, \mathbf{u}(k+i-\hat{n}_u)\right) + \mathbf{e}(k),\ 1 \leqslant i \leqslant P.\end{aligned} \tag{10}$$

The resulting new multistep NMPC design is obtained by minimising the objective function (4) subject to the constraints (6) and

$$\begin{aligned}\mathbf{y}_{\mathrm{p}}(k+i|k) &= \tilde{\mathbf{y}}_m(k+i|k), \quad 1 \leqslant i \leqslant P,\\ \mathbf{y}_{\min} \leqslant \mathbf{y}_{\mathrm{p}}(k+i|k) &\leqslant \mathbf{y}_{\max}, \quad 1 \leqslant i \leqslant P.\end{aligned} \tag{11}$$

The key difference to the DMC-like correcting scheme is that the output feedback error $\mathbf{e}(k)$ is incorporated into the multistep model prediction procedure. Therefore, the plant–model mismatch and/or unmeasured disturbances are continuously compensated in the multistep recursive model prediction propagation (10), and this improves the accuracy of the multistep predictions which in turn results in an enhanced performance of the NMPC algorithm. By contrast, the DMC-like feedback scheme only works in the situation where the plant–model mismatch manifests as an additive output disturbance. We now show that the NMPC algorithm with the proposed correcting scheme can eliminate the steady-state error to achieve offset-free behaviour.

Proposition 1
Assume that

(1) The closed-loop system is stable.
(2) The set point $\mathbf{y}_{\mathrm{sp}}$ is reachable.

Then, for asymptotically constant set points and disturbances, there will be no offset.

Proof
Assumption 1 implies that the closed-loop system can reach an asymptotically stable equilibrium point defined by

$$\mathbf{y}^{\infty} = \mathbf{f}\left(\mathbf{y}^{\infty}, \cdots, \mathbf{y}^{\infty}, \mathbf{u}^{\infty}, \cdots, \mathbf{u}^{\infty}\right),$$

where the superscript $^{\infty}$ denotes the steady state ,whereas $\mathbf{y}^{\infty}$ and $\mathbf{u}^{\infty}$ are the process's steady-state output and input, respectively. From the identified model (2), the model output

$$\mathbf{y}_m^{\infty} = \mathbf{f}_m\left(\mathbf{y}^{\infty}, \cdots, \mathbf{y}^{\infty}, \mathbf{u}^{\infty}, \cdots, \mathbf{u}^{\infty}\right)$$

DOI: 10.1002/acs

is a constant at the process's steady state $\{\mathbf{y}^\infty, \mathbf{u}^\infty\}$. Then, the bias $\mathbf{e}^\infty = \mathbf{y}^\infty - \mathbf{y}_m^\infty \neq \mathbf{0}$ is always a constant. According to the multistep prediction procedure (10), we have the one-step-ahead prediction

$$\begin{aligned}\tilde{\mathbf{y}}_m^\infty(k+1|k) &= \mathbf{f}_m\left(\tilde{\mathbf{y}}_m^\infty(k|k), \cdots, \tilde{\mathbf{y}}_m^\infty(k+1-\hat{n}_y|k), \mathbf{u}^\infty, \cdots, \mathbf{u}^\infty\right) + \mathbf{e}^\infty \\ &= \mathbf{f}_m\left(\mathbf{y}^\infty, \cdots, \mathbf{y}^\infty, \mathbf{u}^\infty, \cdots, \mathbf{u}^\infty\right) + \mathbf{e}^\infty = \mathbf{y}_m^\infty + \mathbf{e}^\infty = \mathbf{y}^\infty,\end{aligned}$$

the two-step-ahead prediction

$$\begin{aligned}\tilde{\mathbf{y}}_m^\infty(k+2|k) &= \mathbf{f}_m\left(\tilde{\mathbf{y}}_m^\infty(k+1|k), \mathbf{y}^\infty, \cdots, \mathbf{y}^\infty, \mathbf{u}^\infty, \cdots, \mathbf{u}^\infty\right) + \mathbf{e}^\infty \\ &= \mathbf{f}_m\left(\mathbf{y}^\infty, \cdots, \mathbf{y}^\infty, \mathbf{u}^\infty, \cdots, \mathbf{u}^\infty\right) + \mathbf{e}^\infty = \mathbf{y}_m^\infty + \mathbf{e}^\infty = \mathbf{y}^\infty,\end{aligned}$$

and recursively the three or more step-ahead predictions

$$\tilde{\mathbf{y}}_m^\infty(k+i|k) = \mathbf{y}^\infty,\ i = 3, \cdots, P.$$

When the process reaches a steady-state,

$$\Delta\mathbf{u}(k+j|k) = \mathbf{u}(k+j|k) - \mathbf{u}(k+j-1|k) = \mathbf{0},\ \forall j \geqslant 0. \tag{12}$$

Thus, the inequality constraints on $\Delta\mathbf{u}(k+j|k)$ in (6) can be removed, and the NMPC formulation described by (4), (11) and (6) is reduced to

$$\begin{aligned}\min_{\Delta\mathbf{u}(k|k),\cdots,\Delta\mathbf{u}(k+M-1|k)} \quad & \sum_{i=1}^{P}\left(\mathbf{y}_{\mathrm{sp}} - \mathbf{y}_{\mathrm{p}}(k+i|k)\right)^{\mathrm{T}}\mathbf{Q}\left(\mathbf{y}_{\mathrm{sp}} - \mathbf{y}_{\mathrm{p}}(k+i|k)\right), \\ \text{s.t.} \quad & \mathbf{y}_{\mathrm{p}}(k+i|k) = \mathbf{y}^\infty,\ 1 \leqslant i \leqslant P, \\ & \mathbf{y}_{\min} \leqslant \mathbf{y}^\infty \leqslant \mathbf{y}_{\max},\ 1 \leqslant i \leqslant P, \\ & \mathbf{u}_{\min} \leqslant \mathbf{u}^\infty \leqslant \mathbf{u}_{\max},\ 1 \leqslant j \leqslant M-1.\end{aligned} \tag{13}$$

Assumption 2 indicates that the set point $\mathbf{y}_{\mathrm{sp}}$ and the corresponding control input $\mathbf{u}_{\mathrm{sp}}$ asymptotically fulfil

$$\begin{aligned}\mathbf{y}_{\min} &\leqslant \mathbf{y}_{\mathrm{sp}} \leqslant \mathbf{y}_{\max}, \\ \mathbf{u}_{\min} &\leqslant \mathbf{u}_{\mathrm{sp}} \leqslant \mathbf{u}_{\max}.\end{aligned} \tag{14}$$

From the solution of (13), we immediately obtain $\mathbf{y}^\infty = \mathbf{y}_{\mathrm{sp}}$. □

Remark 1

The main advantage of our approach is that the computation of the steady-state value of the control input associated with the set point can be avoided. If the set points are not reachable, then the proposed approach minimises the steady-state output difference $\left(\mathbf{y}_{\mathrm{sp}} - \mathbf{y}^\infty\right)^{\mathrm{T}}\mathbf{Q}\left(\mathbf{y}_{\mathrm{sp}} - \mathbf{y}^\infty\right)$. Assumption 1 indicates that the NMPC controller can asymptotically stabilise the process (1) with the given multistep-ahead predictive model (10). This type of assumption is often seen in the literature. For example, this assumption was also adopted in [18, 50, 51], in order to show that the controller considered in [18, 50, 51] yields a zero steady-state offset.

Remark 2

Under the same assumptions as given in Proposition 1, the DMC-like method cannot guarantee the same offset-free control performance. This may be explained as follows. When the process reaches the steady state $\{\mathbf{y}^\infty, \mathbf{u}^\infty\}$, from (3) and (9), we have the error-corrected one-step-ahead prediction

$$\mathbf{y}_{\mathrm{p}}(k+1|k) = \mathbf{y}_m^\infty(k+1|k) + \mathbf{e}^\infty = \mathbf{f}_m\left(\mathbf{y}^\infty, \cdots, \mathbf{y}^\infty, \mathbf{u}^\infty, \cdots, \mathbf{u}^\infty\right) + \mathbf{e}^\infty = \mathbf{y}_m^\infty + \mathbf{e}^\infty = \mathbf{y}^\infty,$$

the error-corrected two-step-ahead prediction

$$\mathbf{y}_{\mathrm{p}}(k+2|k) = \mathbf{f}_m\left(\mathbf{y}_m^\infty, \mathbf{y}^\infty, \cdots, \mathbf{y}^\infty, \mathbf{u}^\infty, \cdots, \mathbf{u}^\infty\right) + \mathbf{e}^\infty \neq \mathbf{y}^\infty$$

DOI: 10.1002/acs

and the error-corrected three or more step-ahead predictions

$$\mathbf{y}_{\mathrm{p}}(k+i|k) \neq \mathbf{y}^{\infty}, i = 3, \cdots, P.$$

Thus, the NMPC formulation described by (4), (9) and (6) is reduced to

$$\begin{array}{ll} \min\limits_{\Delta\mathbf{u}(k|k),\cdots,\Delta\mathbf{u}(k+M-1|k)} & \sum\limits_{i=1}^{P} \left(\mathbf{y}_{\mathrm{sp}} - \mathbf{y}_{\mathrm{p}}(k+i|k)\right)^{\mathrm{T}} \mathbf{Q} \left(\mathbf{y}_{\mathrm{sp}} - \mathbf{y}_{\mathrm{p}}(k+i|k)\right), \\ \text{s.t.} & \mathbf{y}_{\mathrm{p}}(k+i|k) = \mathbf{y}_{m}^{\infty}(k+i|k) + \mathbf{e}^{\infty},\ 1 \leqslant i \leqslant P, \\ & \mathbf{y}_{\min} \leqslant \mathbf{y}_{\mathrm{p}}(k+i|k) \leqslant \mathbf{y}_{\max},\ 1 \leqslant i \leqslant P, \\ & \mathbf{u}_{\min} \leqslant \mathbf{u}^{\infty} \leqslant \mathbf{u}_{\max},\ 1 \leqslant j \leqslant M-1. \end{array} \quad (15)$$

It then becomes obvious that the solution of the optimisation problem (15) can only be obtained in the sense of least-squares error, and in general, the offset will occur, namely, $\mathbf{y}^{\infty} \neq \mathbf{y}_{\mathrm{sp}}$.

Remark 3

In practical applications of MPC, if the desired set point changes significantly or large persistent disturbances occur, the feasibility of the controller may be lost. This is because in these cases, there may be a conflict between the constraints (6) and the constraints (11) that may turn the control problem infeasible. Two approaches can be employed to recover the feasibility of the NMPC whenever the controller feasibility is lost due to large set-point changes or persistent disturbances.

The first approach introduces an artificial set point to the MPC problem as a new decision variable [52]. The distance between the artificial set point $\hat{\mathbf{y}}_{\mathrm{sp}} \in \mathbb{R}^{m_y}$ and the real one $\mathbf{y}_{\mathrm{sp}}$ is then penalised in the cost function, and the resulting optimisation problem is expressed as

$$\begin{aligned} \min_{\Delta\mathbf{u}(k|k),\cdots,\Delta\mathbf{u}(k+M-1|k),\hat{\mathbf{y}}_{\mathrm{sp}}} & \sum_{i=1}^{P} \left(\hat{\mathbf{y}}_{\mathrm{sp}} - \mathbf{y}_{\mathrm{p}}(k+i|k)\right)^{\mathrm{T}} \mathbf{Q} \left(\hat{\mathbf{y}}_{\mathrm{sp}} - \mathbf{y}_{\mathrm{p}}(k+i|k)\right) \\ & + \sum_{j=0}^{M-1} \left(\Delta\mathbf{u}(k+j|k)\right)^{\mathrm{T}} \mathbf{R} \Delta\mathbf{u}(k+j|k) + \left(\hat{\mathbf{y}}_{\mathrm{sp}} - \mathbf{y}_{\mathrm{sp}}\right)^{\mathrm{T}} \mathbf{Q}_{\mathrm{s}} \left(\hat{\mathbf{y}}_{\mathrm{sp}} - \mathbf{y}_{\mathrm{sp}}\right), \end{aligned} \quad (16)$$

subject to the constraints (11) and (6), where $\mathbf{Q}_{\mathrm{s}}$ is the weighting matrix for penalising the difference between the artificial set point and the actual set point. The introduction of the artificial set point as the new decision variable can explicitly address the feasibility of the controller and ensure the convergence to the target if admissible. Furthermore, the domain of attraction of this controller is potentially larger than those of reference governors and standard predictive controllers [53].

In the second approach, the soft constraints are introduced to extend the constraint handling capabilities of MPC [54, 55]. The output predictions are softened by means of slack variables and the MPC optimisation problem is reformulated as following

$$\begin{aligned} \min_{\Delta\mathbf{u}(k|k),\cdots,\Delta\mathbf{u}(k+M-1|k),\boldsymbol{\varepsilon},\varepsilon_{\min},\varepsilon_{\max}} & \sum_{i=1}^{P} \left(\mathbf{y}_{\mathrm{sp}} - \mathbf{y}_{\mathrm{p}}(k+i|k) - \varepsilon\right)^{\mathrm{T}} \mathbf{Q} \left(\mathbf{y}_{\mathrm{sp}} - \mathbf{y}_{\mathrm{p}}(k+i|k) - \varepsilon\right) \\ & + \sum_{j=0}^{M-1} \left(\Delta\mathbf{u}(k+j|k)\right)^{\mathrm{T}} \mathbf{R} \Delta\mathbf{u}(k+j|k) + \varepsilon^{\mathrm{T}} \mathbf{Q}_{\varepsilon} \varepsilon + \rho_{\min} \|\varepsilon_{\min}\|^2 + \rho_{\max} \|\varepsilon_{\max}\|^2, \end{aligned} \quad (17)$$

subject to the constraints (6) and

$$\begin{aligned} \mathbf{y}_{\mathrm{p}}(k+i|k) = \tilde{\mathbf{y}}_{m}(k+i|k), &\quad 1 \leqslant i \leqslant P, \\ \mathbf{y}_{\min} - \varepsilon_{\min} \leqslant \mathbf{y}_{\mathrm{p}}(k+i|k) \leqslant \mathbf{y}_{\max} + \varepsilon_{\max}, &\quad 1 \leqslant i \leqslant P, \\ \varepsilon_{\min} \geqslant \mathbf{0},\ \varepsilon_{\max} \geqslant \mathbf{0}, & \end{aligned} \quad (18)$$

where $\varepsilon \in \mathbb{R}^{m_y}$ is a slack variable, $\varepsilon_{\min}$ and $\varepsilon_{\max} \in \mathsf{R}^{m_y}$ are the lower-bound and upper-bound slack variables, respectively, $\mathbf{Q}_{\varepsilon}$ is the weighting matrix for the slack variable ε and $\rho_{\min}$ and $\rho_{\max} > 0$ are the two weightings for the lower-bound and upper-bound slack variables, respectively. With the

DOI: 10.1002/acs

help of the slack variables, the original hard constraint (11) posed on the magnitude of the output variable can be temporarily violated. This enlarges the admissible set and prevents the infeasibility of the solution from happening. The degree of output constraint violation is minimised by the last three terms of the objective function (17). In addition, it provides a flexible mechanism for shaping the transient response by tuning $\mathbf{Q}$ and $\mathbf{Q}_\varepsilon$. The controller obtained from the solution to the problems (17), (6) and (18) shares the same properties related to the feasibility of the set-point tracking problem as the controller defined in (16), (6) and (11).

4. SIMULATION STUDY

The CSTR [27, 29] was employed to compare the closed-loop performance of several MPC algorithms and to demonstrate that the proposed NMPC scheme can achieve offset-free control in the presence of significant plant–model mismatch and unmeasured disturbances. A Van der Vusse chemical reaction takes place in the CSTR with a cooling jacket. The main reaction is given by the transformation of cyclopentadiene, $\mathcal{A}$, to the product cyclopentenol, $\mathcal{B}$, which in turn produces cyclopentanediol, $\mathcal{C}$, in an unwanted consecutive reaction. The initial reactant, $\mathcal{A}$, also reacts in an unwanted parallel reaction to give the by-product dicyclopentadiene, $\mathcal{D}$. Symbolically, this chemical reaction is described as

$$\begin{aligned} &\mathcal{A} \xrightarrow{\kappa_1} \mathcal{B} \xrightarrow{\kappa_2} \mathcal{C} \\ &2\mathcal{A} \xrightarrow{\kappa_3} \mathcal{D} \end{aligned}$$

The dynamics of the reactor can be described by the following nonlinear differential equations that are derived from the component balances for substances $\mathcal{A}$ and $\mathcal{B}$ and from the energy balances for the reactor and cooling jacket

$$\begin{aligned} \dot{C}_a &= q\,(C_{a0} - C_a) - \kappa_1(T)C_a - \kappa_3(T)C_a^2, \\ \dot{C}_b &= -qC_b + \kappa_1(T)C_a - \kappa_2(T)C_b, \\ \dot{T} &= q(T_0 - T) - \frac{1}{\rho C_P}\left(\kappa_1(T)C_a\Delta H_1 + \kappa_2(T)C_b\Delta H_2 + \kappa_3(T)C_a^2\Delta H_3\right) \\ &\quad + \frac{\kappa_w A_R}{\rho C_P V_R}\left(T_K - T\right), \\ \dot{T}_K &= \frac{1}{m_K C_{PK}}\left(Q_K + \kappa_w A_R(T - T_K)\right). \end{aligned} \tag{19}$$

The reaction velocities κ_i are assumed to depend on the temperature via the Arrhenius law

$$\kappa_i(T) = \kappa_{i0}\exp\left(-\frac{E_i}{R(T + 273.15)}\right), i = 1, 2, 3. \tag{20}$$

The states of the system consist of the concentrations of components $\mathcal{A}$ and $\mathcal{B}$, $C_a \geqslant 0$ and $C_b \geqslant 0$, as well as the temperatures, T and T_K, occurring in the reactor and cooling jacket, respectively. This is a two-input two-output process. The two controlled variables are $y_1 = C_b$ and $y_2 = T$, the concentration of substance $\mathcal{B}$ and the temperature in the reactor, whereas the two control inputs are $u_1 = q$ and $u_2 = Q_K$, the flow rate (scaled to the volume of the reactor) and the cooling power, which are subject to the constraints

$$q \in [3,\ 35]h^{-1},\ Q_K \in [-9000,\ 0] \text{ kJ/h},\ |\Delta q| \leqslant 5h^{-1},\ |\Delta Q_K| \leqslant 2000 \text{ kJ/h}.$$

The values for the physical and chemical parameters in (19) and (20) are listed in Table I.

The reactor exhibits input multiplicities, that is, more than one set of the manipulated variable values can produce an identical steady-state output. Input multiplicities exist when the steady-state gain matrix becomes singular in the operating region. During the actual operation of the plant, it is always required to operate at the optimal operating point that can produce the maximum concentration of $\mathcal{B}$. Although control at such an operating point appears to be economically the most

DOI: 10.1002/acs

Table I. Physical and chemical parameters of the CSTR process.

Name of parameter	Symbol	Value of parameter
Pre-exponential factor	κ_{10}	$1.287 \times 10^{12}\ h^{-1}$
Pre-exponential factor	κ_{20}	$1.287 \times 10^{12}\ h^{-1}$
Pre-exponential factor	κ_{30}	$9.043 \times 10^{9}\ h^{-1}$
Activation energy for reaction κ_1	E_1	81.1344 kJ/mol
Activation energy for reaction κ_2	E_2	81.1344 kJ/mol
Activation energy for reaction κ_3	E_3	71.1712 kJ/mol
Enthalpies of reaction κ_1	ΔH_1	4.2 kJ/(mol·l)
Enthalpies of reaction κ_2	ΔH_2	−11.0 kJ/(mol·l)
Enthalpies of reaction κ_3	ΔH_3	−41.85 kJ/(mol·l)
Density	ρ	0.9342 kg/l
Heat capacity	C_P	3.01 kJ/(kg·K)
Heat transfer coefficient for cooling jacket	κ_w	4032 kJ/(h·m^2·K)
Surface of cooling jacket	A_R	0.215 m^2
Reactor volume	V_R	0.01 m^3
Coolant mass	m_K	5.0 kg
Heat capacity of coolant	C_{PK}	2.0 kJ/(kg·K)
Universal gas constant	R	8.314 J/(mol·K)
Concentration of initial reactant	C_{a0}	5.10 mol/l
Feed temperature	T_0	104.9 °C

desirable, the resulting control problem is difficult to handle because there exists a singularity at the optimum operating point. The existence of such singular points renders the task of controlling a system exhibiting input multiplicities extremely difficult [56].

4.1. *Modelling and model evaluation*

A dynamic SVR model with the NARX structure (2) was used to model the CSTR on the basis of an input–output data set obtained from the CSTR process. The model took the form

$$y_{m,i}(k) = f_{m,i}(y_1(k-1), y_2(k-1), u_1(k-1), u_2(k-1)),\ i = 1, 2,$$

with the input and output lags set to $\hat{n}_y = \hat{n}_u = 1$. The tuning parameters of the SVR model with the Gaussian kernel were chosen as follows: the maximum tolerable error $\chi = 0.05$, the regularisation parameter $C = 50$ and the kernel width $\sigma = 0.005$ were used for identifying $f_{m,1}$, whereas $\chi = 0.05$, $C = 20$ and $\sigma = 0.01$ were used for identifying $f_{m,2}$. In the simulation, the sampling period was set to 18 s, and 800 input–output data were gathered by injecting the random step signals with the uniform distributions in $[3,\ 35]h^{-1}$ and $[-9000,\ 0]$ kJ/h as the control inputs q and Q_K, respectively, with the switching probability of 0.2. The first 200 training data were used to train the two SVR models with LIBSVM toolbox [57], which led to 43 support vectors for $f_{m,1}$ and 31 support vectors for $f_{m,2}$. The last 600 data points were employed to validate the two obtained models.

Figure 1 compares the two process outputs with those of the two identified SVR models over both the training and validation data sets, where it is observed that the two one-step-ahead prediction curves almost coincide with the actual process outputs. The root mean squares error (RMSE) between the actual process output $y_i(k)$ and the j-step-ahead model prediction $y_{m,i}(k + j|k)$

$$\mathrm{RMSE}_i(j) = \sqrt{\sum_{k=1}^{N} (y_i(k) - y_{m,i}(k + j|k))^2 / N}, i = 1, 2$$

was evaluated over the validation data set, and the values of RMSE obtained for the two process outputs C_b and T, respectively, are listed in Table II. The one-step-ahead RMSE values given in Table II together with the results of Figure 1 indicate that the two identified SVR models achieved very small one-step-ahead prediction errors. However, the multistep predictive error accumulated

DOI: 10.1002/acs

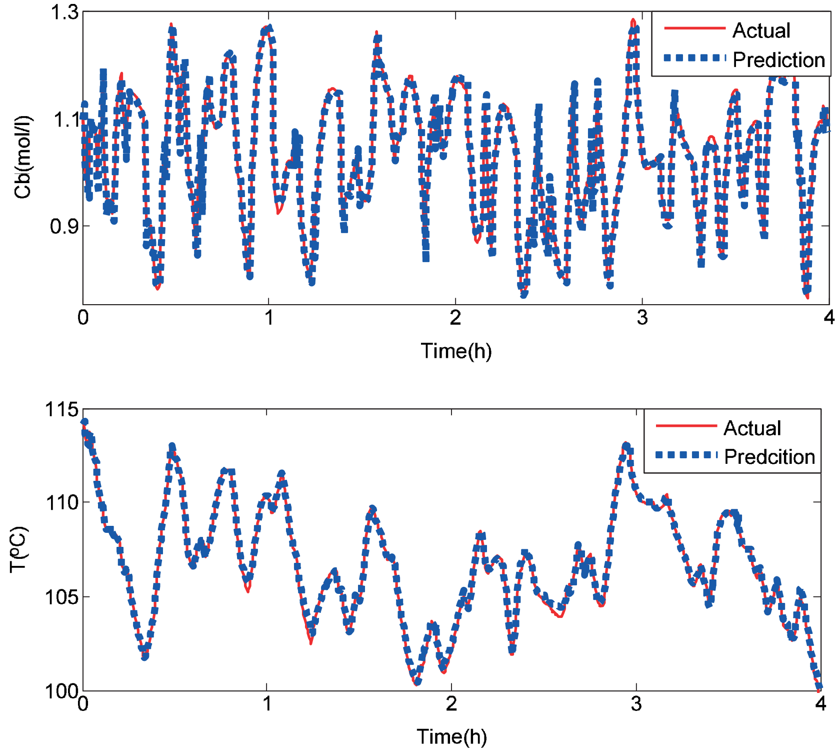

Figure 1. Comparison of the actual CSTR process outputs (solid) and the one-step-ahead predictions from the identified SVR models (dashed) over the training (first 200 points) and validation (last 600 points) data. The sampling period is 18 s.

Table II. RMSE between the actual process output and the j-step-ahead model prediction for the two process outputs C_b and T.

j	1	2	3	4	5	6	7	8
RMSE for C_b	0.0214	0.0277	0.0320	0.0353	0.0390	0.0402	0.0413	0.0422
RMSE for T	0.2220	0.4245	0.6171	0.7947	0.9573	1.1033	1.2355	1.3542

and increased as the prediction horizon increased. This can be clearly observed from Table II. Figure 2 compares the steady-state behaviours of the process outputs C_b and T as the function of the control input q, when fixing the other control input to $Q_K = -1118$ kJ/h, with the steady-state behaviours generated by the identified SVR model. It is observed from Figure 2 that the steady-state operating locus of the actual plant displays a gain change at the flow rate $q = 14.19h^{-1}$, which corresponds to the operation point $C_b = 1.09$ mol/l and $T = 114.2$ °C. By contrast, the gain change for the SVR model occurs at $q = 6.88h^{-1}$, and the model steady-state outputs at this point are $C_b = 1.171$ mol/l and $T = 113.6$ °C. The existence of such significant plant–model mismatch served well our purpose of testing the performance of various NMPC schemes in the presence of plant–model mismatch.

4.2. Set-point tracking

The three NMPC schemes implemented in the simulation study are first summarised:

- *NMPC1*: the NMPC algorithm based on the 'perfect' process model without any plant–model mismatch. This served as the 'ideal' NMPC algorithm.
- *NMPC2*: the NMPC algorithm based on the proposed correcting scheme. This was the proposed 'new' NMPC algorithm.

DOI: 10.1002/acs

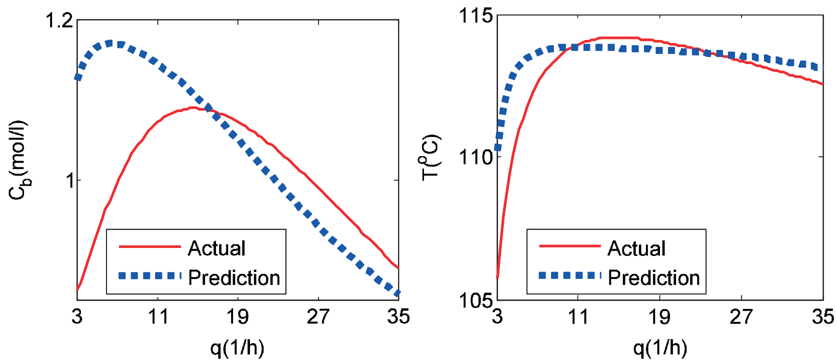

Figure 2. Steady-state behaviours of the actual CSTR process (solid) and the identified SVR models (dashed) as the function of the control input q, when setting the other control input to $Q_K = -1118$ kJ/h.

- *NMPC3*: the NMPC algorithm based on the DMC-like correcting scheme. This was the 'most widely' implemented NMPC algorithm.

The identified SVR model as given in Section 4.1 was used for designing the NMPC2 and NMPC3. The prediction horizon and the control horizon were set to $P = 13$ and $M = 1$, respectively. The output and input weighting matrices in the cost function were chosen to be $\mathbf{Q} = \text{diag}\{200, 10\}$ and $\mathbf{R} = \text{diag}\{1, 0.02\}$, respectively. An artificial set point $\hat{\mathbf{y}}_{sp} \in \mathbb{R}^2$ was introduced to the NMPC optimisation problem to ensure the feasibility of the NMPC during the change of set point. The weighting matrix for penalising the difference between the artificial set point and the actual set point was set to $\mathbf{Q}_s = \text{diag}\{400, 50\}$. Ability of the proposed NMPC scheme to achieve steady-state offset-free control was investigated when the CSTR went through a series of set-point changes:

$$\begin{aligned} t &= 0-0.6 \text{ h:} && \text{process set point (1.09 mol/l, 114.2 °C)} \\ t &= 0.6-1.2 \text{ h:} && \text{process set point (1.06 mol/l, 113.0 °C)} \\ t &= 1.2-1.8 \text{ h:} && \text{process set point (1.09 mol/l, 114.2 °C)} \end{aligned}$$

Figures 3–5 illustrate the closed-loop performance of the three NMPC controllers for set-point tracking, where the performance of the NMPC1 serves as a lower bound. As can be seen from Figure 5, the output feedback error $\mathbf{e}(k) = \mathbf{0}$ for the NMPC1 because the exact process model was used, whereas $\mathbf{e}(k) \neq \mathbf{0}$ for the other two MPC systems as the plant–model mismatch existed in these two cases. Whereas the output feedback error is the difference between the actual process output and the model output, which reflects the plant–model mismatch, the offset error is the difference between the actual process output and its set point, and it is highly desired that a control system can achieve the steady-state zero offset error. From Figure 3, it can be seen that the set-point tracking performance of the NMPC2 with the new multistep prediction procedure (10) was very close to the ideal performance of the NMPC1. This demonstrates that the proposed NMPC2 can effectively correct the plant–model mismatch to achieve offset-free control. By contrast, the NMPC3 with the DMC-type feedback correction could not achieve the offset-free control, as can be clearly seen from Figure 3. Note that the steady-state gain of the CSTR reduces to zero at the set point (1.09 mol/l, 114.2 °C), which can lead to controller output fluctuations at the neighbourhood of this point. The ability of the proposed correcting scheme to 'predict' the system dynamics close to the singular points accurately, however, ensured that the control input fluctuations were not large even when the process's steady-state gain was close to zero. By contrast, the controller response of the NMPC3 exhibited large overshoot behaviour, as is clearly shown in Figure 4.

The sum of squared errors (SSE) between the desired set point and the actual process output over the sampling interval $[N_1, N_2]$, defined as

$$\text{SSE}_i = \sum_{k=N_1}^{N_2} \left(y_{sp,i} - y_i(k)\right)^2, \; i = 1, 2,$$

DOI: 10.1002/acs

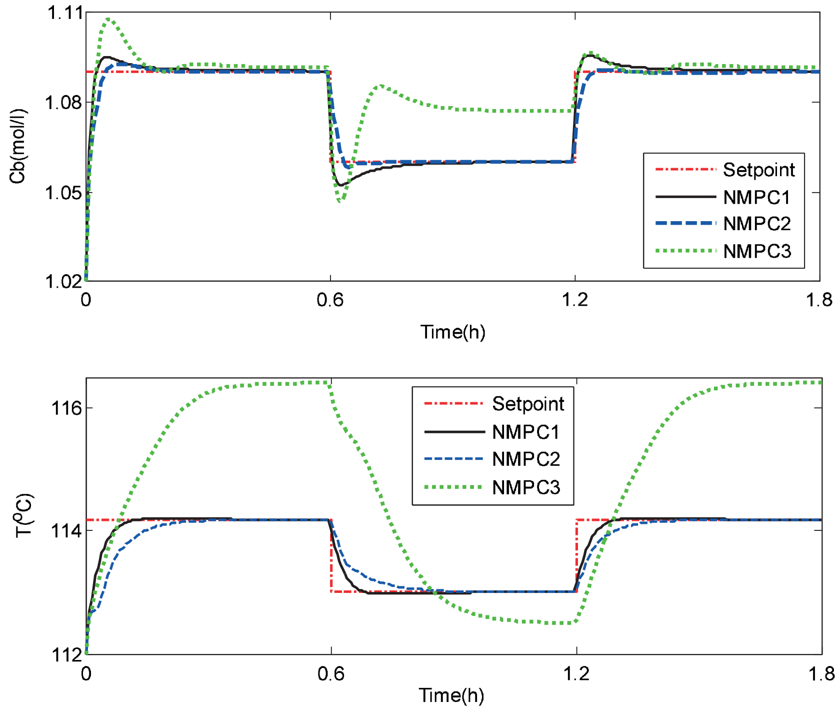

Figure 3. Set-point tracking performance of various NMPC controllers: process output $\mathbf{y}(k)$.

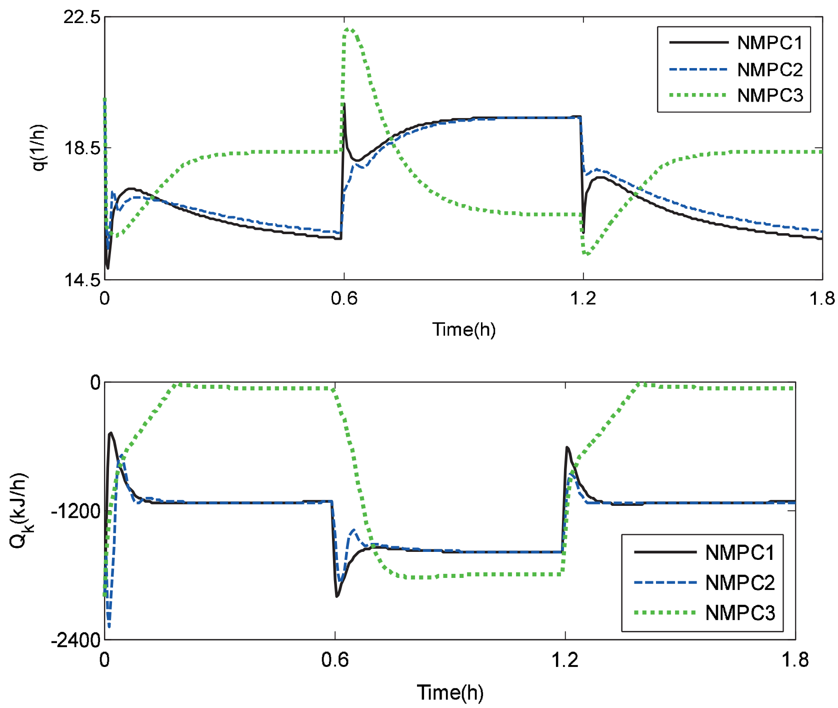

Figure 4. Set-point tracking performance of various NMPC controllers: controller output $\mathbf{u}(k)$.

was used to quantify the offset error performance of a controller. Table III compares the SSE values over the six sampling intervals of each length 0.3 h for the three NMPC algorithms investigated. As can be seen from Table III, the NMPC3 cannot achieve offset-free control. By contrast, the NMPC2

DOI: 10.1002/acs

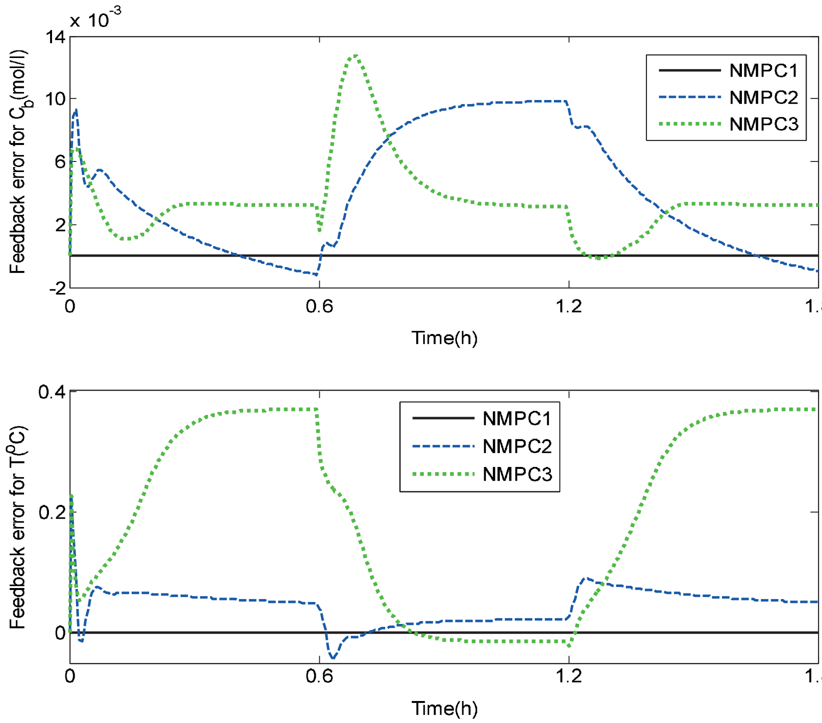

Figure 5. Set-point tracking performance of various NMPC controllers: output feedback error $\mathbf{e}(k)$.

Table III. Comparison of the SSEs between the set point and the actual process output for the three NMPC controllers in set-point tracking.

	Sampling interval (h)	SSE for C_b	SSE for T
NMPC1	0 – 0.3	0.0083	15.6026
	0.3 – 0.6	$1.3689e-4$	1.0046
	0.6 – 0.9	$7.7499e-4$	3.5356
	0.9 – 1.2	$3.7521e-7$	$1.8926e-4$
	1.2 – 1.5	$5.9986e-4$	4.0840
	1.5 – 1.8	$8.7761e-6$	0.0047
NMPC2	0 – 0.3	0.0101	29.4195
	0.3 – 0.6	$5.8316e-4$	1.2510
	0.6 – 0.9	0.0014	7.3578
	0.9 – 1.2	$4.3571e-7$	0.0025
	1.2 – 1.5	0.0011	7.1895
	1.5 – 1.8	$6.4498e-6$	$1.8934e-4$
NMPC3	0 – 0.3	0.0129	109.6343
	0.3 – 0.6	$6.1421e-4$	299.5152
	0.6 – 0.9	0.0213	164.5560
	0.9 – 1.2	0.0181	11.4718
	1.2 – 1.5	$5.3736e-4$	97.7208
	1.5 – 1.8	$1.7602e-4$	288.0552

can realise the offset-free control after 0.3 h of each set-point change. This again demonstrates that the new NMPC controller can effectively utilise the available output feedback error information to remove the influence of plant–model mismatch in the proposed multistep-ahead predictive procedure. The results of Table III also confirm that the set-point tracking performance of the NMPC2 is close to that of the ideal NMPC1.

DOI: 10.1002/acs

4.3. Unmeasured disturbance rejection

During the operation of a chemical process, unmeasured disturbances may arise owing to various factors, such as changes in the quality of raw material or interactions between different plant units. We evaluated the ability of the proposed NMPC formulation, the NMPC2, for disturbance rejection. In the simulation, the feed of the reactor was assumed to come from an upstream unit, and the feed temperature T_0 could vary in the range [100 °C, 115 °C]. The objective of this part of simulation was to shift the process from an initial operation point $(C_a, C_b, T, T_K) = (1 \text{ mol/l}, 0.5 \text{ mol/l}, 100\ ^\circ\text{C}, 100\ ^\circ\text{C})$ at $k = 0$ to the nominal optimal operating point (2.14 mol/l, 1.09 mol/l, 114.2 °C, 112.9 °C) with the set point $C_b = 1.09$ mol/l and $T = 114.2$ °C when the process was subject to the unmeasured disturbance described by

$$T_0(k) = \begin{cases} 104.9\ ^\circ\text{C}, & k < 20, \\ 104.9 + \frac{k-20}{30} \times 5.1\ ^\circ\text{C}, & 20 \leqslant k < 50, \\ 110.0\ ^\circ\text{C}, & k \geqslant 50. \end{cases}$$

In addition, the measurements of the process outputs, C_b and T, were corrupted by the zero-mean Gaussian white noise signals with the standard deviations of 0.08 and 0.3, respectively. This control problem was especially challenging, as the controller attempted to drive the reactor to the operation point that is characterised by a change of sign in the steady-state gain. Moreover, the process suffered from unmeasured disturbance, and the measurements were corrected by noise.

Closed-loop performance of the three NMPC controllers are depicted in Figures 6–8. The tracking results shown in Figure 6 confirm that the performance of the NMPC2 was still close to that of the ideal NMPC1, under the unmeasured disturbance and measurement noise. It can be observed from Figure 7 that, for the NMPC1 and NMPC2, the manipulated variables Q_K decreased appropriately in responding to the effects of the ramp disturbance $T_0(k)$ for $20 \leqslant k < 50$. For this challenging control problem, the process outputs of the closed-loop systems under the controllers NMPC1 and NMPC2 achieved relative smooth transitions to the optimal operation point, and they remained

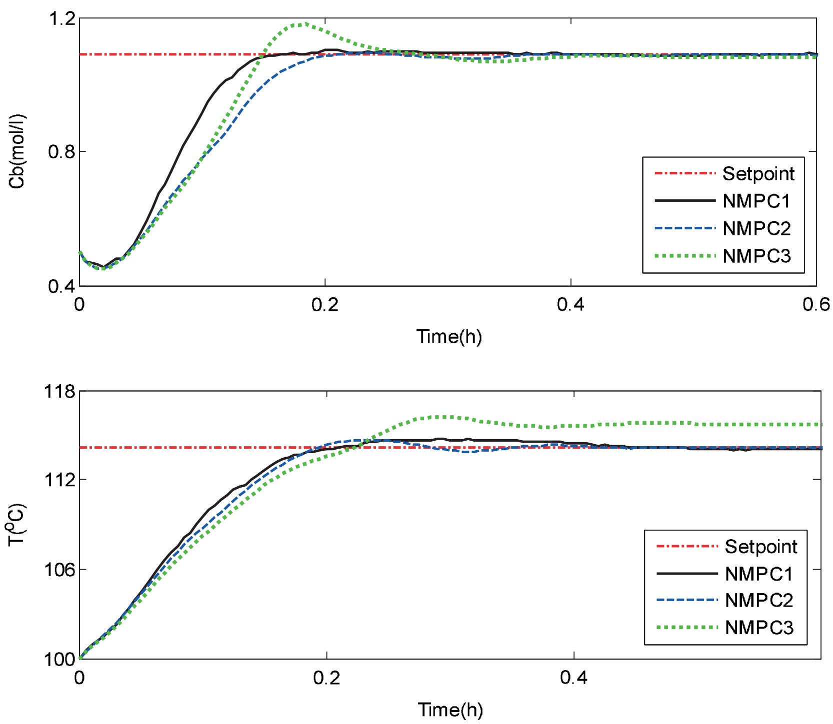

Figure 6. Disturbance rejection performance of various NMPC controllers: process output $\mathbf{y}(k)$.

DOI: 10.1002/acs

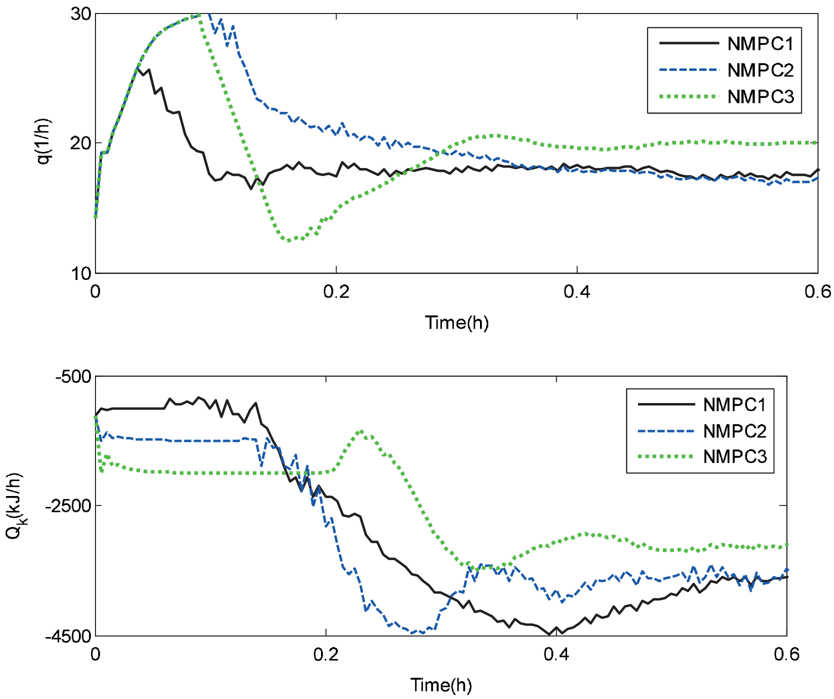

Figure 7. Disturbance rejection performance of various NMPC controllers: controller output $\mathbf{u}(k)$.

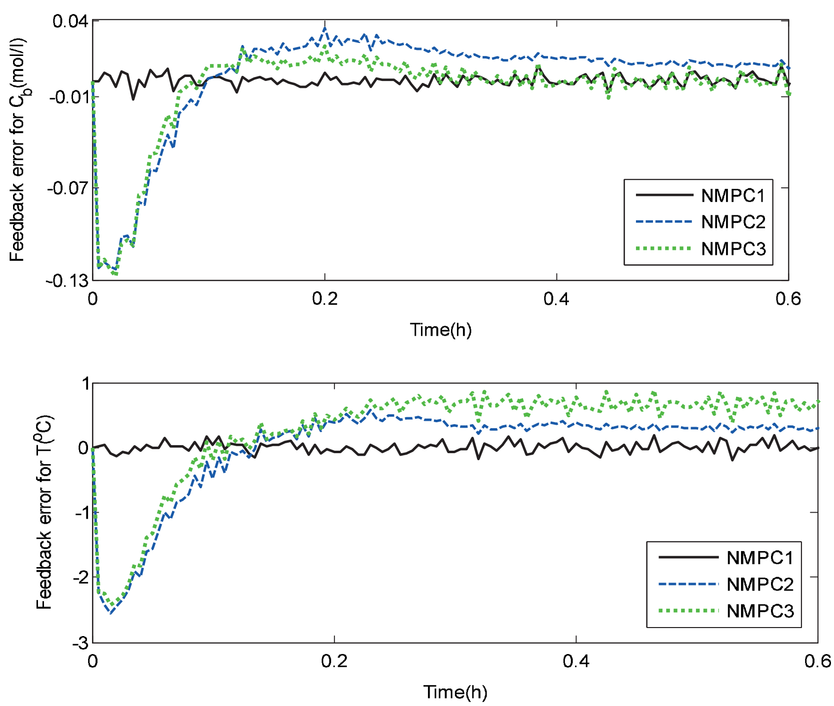

Figure 8. Disturbance rejection performance of various NMPC controllers: output feedback error $\mathbf{e}(k)$.

at the set point without obvious steady-state error. The NMPC3, by contrast, exhibited overshoot behaviour and experienced clear steady-state error for the set point T. As the process output measurements were corrupted by the random noise, the output feedback error was no longer

DOI: 10.1002/acs

Table IV. Comparison of the SSEs between the set point and the actual process output for the three NMPC controllers, averaged over 50 runs, in disturbance rejection.

	Sampling interval (h)	SSE for C_b	SSE for T
NMPC1	0 – 0.3	5.2780	$2.2183e+3$
	0.3 – 0.6	$6.0816e-4$	0.4160
NMPC2	0 – 0.3	6.1125	$2.3207e+3$
	0.3 – 0.6	$6.4123e-4$	0.5139
NMPC3	0 – 0.3	6.2801	$2.5753e+3$
	0.3 – 0.6	0.0046	192.7004

identical to zero for the ideal NMPC1, which is confirmed in Figure 8. The simulation was then repeated for 50 runs, and the means of the SSEs over the two sampling intervals, [0, 0.3] and [0.3, 0.6] h, are listed in Table IV for the three NMPC systems.

5. CONCLUSIONS

The performance of the standard NMPC is critically affected by the accuracy of the prediction model employed. However, an accurate process model can rarely be found with affordable efforts. Moreover, in practical applications, unmeasured disturbances and changes in the process parameters inevitably result in significant mismatch in the plant and model behaviours. Under these circumstances, most current NMPC implementations often experience steady-state offset errors, namely, a persistent discrepancy between the desired set-point value and the actual output of the process, leading to a significant degradation in the closed-loop performance. In this contribution, a methodology for achieving steady-state offset-free control has been proposed for the NMPC implementation under significant plant–model mismatch and/or unmeasured disturbances. The methodology is based on incorporating the available output feedback error in the multistep recursive prediction propagation, which explicitly accounts for the uncertainties arising from the plant–model mismatch and unmeasured disturbances. In the proposed multistep prediction procedure, the prediction can effectively correct itself over the prediction horizon based only on the previous output feedback error information. We have proved that the new NMPC formulation based on the proposed correcting scheme is capable of realising steady-state offset-free control. The effectiveness of the proposed NMPC scheme has been demonstrated in the simulation study involving control of the CSTR process. The results obtained have confirmed that the new NMPC formulation with the proposed multistep prediction procedure is able to achieve the satisfactory closed-loop performance and offset-free control even in the presence of significant plant–model mismatch and unmeasured disturbances.

ACKNOWLEDGEMENTS

This work was supported by the National Natural Science Foundation of China under grant 60974008 and the National High Technology Research and Development Program of China under grant 2007AA04Z193. The authors would like to thank anonymous reviewers for their constructive comments that strengthened the manuscript significantly.

REFERENCES

1. Qin SJ, Badgwell TA. A survey of industrial model predictive control technology. *Control Engineering Practice* 2003; **11**(7):733–764.
2. Engell S. Feedback control for optimal process operation. *Journal of Process Control* 2007; **17**(3):203–219.
3. Bequette BW. Non-linear model predictive control: a personal retrospective. *Canadian Journal of Chemical Engineering* 2007; **85**(4):408–415.
4. Magni L, Raimondo MD, Allgöwer F (eds). *Nonlinear Model Predictive Control: Towards New Challenging Applications*, Lecture Notes in Control and Information Sciences, Vol. 384. Springer-Verlag: Berlin, 2009.

5. Badwe AS, Patwardhan RS, Shah SC, Patwardhan SC, Gudi RD. Quantifying the impact of model-plant mismatch on controller performance. *Journal of Process Control* 2010; **20**(4):408–425.
6. Tenny MJ, Rawlings JB, Wright SJ. Closed-loop behavior of nonlinear model predictive control. *AIChE Journal* 2004; **50**(9):2142–2154.
7. Faanes A, Skogestad S. Offset-free tracking of model predictive control with model mismatch: experimental results. *Industrail & Engineeering Chemistry Research* 2005; **44**(11):3966–3972.
8. Gerkšič S, Strmčnik S, van den Boom T. Feedback action in predictive control: an experimental case study. *Control Engineering Practice* 2008; **16**(3):321–332.
9. Magni L, De Nicolao G, Scattolini R. Output feedback and tracking of nonlinear systems with model predictive control. *Automatica* 2001; **37**(10):1601–1607.
10. González AH, Adam EJ, Marchetti JL. Conditions for offset elimination in state space receding horizon controllers: a tutorial analysis. *Chemical Engineering and Processing: Process Intensification* 2008; **47**(12):2184–2194.
11. Maeder U, Morari M. Offset-free reference tracking with model predictive control. *Automatica* 2010; **46**(9):1469–1476.
12. Rao CV, Rawlings JB. Steady states and constraints in model predictive control. *AICHE Journal* 1999; **45**(6):1266–1278.
13. Muske KR, Badgwell TA. Disturbance modeling for offset-free linear model predictive control. *Journal of Process Control* 2002; **12**(5):617–632.
14. Pannocchia G, Rawlings JB. Disturbance models for offset-free model predictive control. *AIChE Journal* 2003; **49**(2):426–437.
15. Pannocchia G. Robust disturbance modeling for model predictive control with application to multivariable ill-conditioned processes. *Journal of Process Control* 2003; **13**(8):693–701.
16. Pannocchia G, Bemporad A. Combined design of disturbance model and observer for offset-free model predictive control. *IEEE Transactions on Automatic Control* 2007; **52**(6):1048–1053.
17. Huang R, Patwardhan SC, Biegler LT. Robust extended Kalman filter based nonlinear model predictive control formulation. *Proceeding of Joint 48th IEEE CDC and 28th CCC*, Shanghai, China, December 15–18, 2009; 8046–8051.
18. Huang R, Biegler LT, Patwardhan SC. Fast offset-free nonlinear model predictive control based on moving horizon estimation. *Industrial & Engineering Chemistry Research* 2010; **49**(17):7882–7890.
19. Lee LM, Lee JH. Approximate dynamic programming-based approaches for input-output data-driven control of nonlinear processes. *Automatica* 2005; **41**(7):1281–1288.
20. Psichogios DM, Ungar LH. Direct and indirect model based control using artificial neural networks. *Industrail & Engineeering Chemistry Research* 1991; **30**(12):2564–2573.
21. Chu JZ, Tsai PF, Tsai WY, Jang SS, Shieh SS, Lin PH, Jiang SJ. Multi-step model predictive control based on artificial neural network. *Industrail & Engineeering Chemistry Research* 2003; **42**(21):5215–5228.
22. Lu CH, Tsai CC. Generalized predictive control using recurrent fuzzy neural networks for industrial processes. *Journal of Process Control* 2007; **17**(1):83–92.
23. Zhang T, Feng G, Zeng XJ. Output tracking of constrained nonlinear processes with offset-free input-to-state stable fuzzy predictive control. *Automatica* 2009; **45**(4):900–909.
24. Uppal A, Ray WH, Poore AB. On the dynamic behavior of continuous stirred tank reactors. *Chemical Engineering Science* 1974; **29**(4):967–985.
25. Calvet JP, Arkun Y. Feedforward and feedback linearization of nonlinear systems and its implementation using internal model control (IMC). *Industrail & Engineeering Chemistry Research* 1988; **27**(10):1822–1831.
26. Hernández E, Arkun Y. Study of the control-relevant properties of back propagation neural network models of nonlinear dynamical systems. *Computers & Chemical Engineering* 1992; **16**(4):227–240.
27. Chen H, Kremling A, Allgöwer F. Non-linear predictive control of a benchmark, CSTR. *Proceeding of 3rd European Control Conference*, Rome, Italy, September 5–8, 1995; 3247–3252.
28. Zhan J, Ishida M. The multi-step predictive control of nonlinear SISO processes with a neural model predictive control (NMPC) method. *Computers & Chemical Engineering* 1997; **21**(2):201–210.
29. Chen H, Allgöwer F. A computationally attractive nonlinear predictive control scheme with guaranteed stability for stable systems. *Journal of Process Control* 1998; **8**(5–6):475–485.
30. Venkateswarlu C, Rao KV. Dynamic recurrent radial basis function network model predictive control of unstable nonlinear processes. *Chemical Engineering Science* 2005; **60**(23):6718–6732.
31. Magni L, Scattolini R. On the solution of the tracking problem for non-linear systems with MPC. *International Journal of Systems Science* 2005; **36**(8):477–484.
32. Magni L. On robust tracking with non-linear model predictive control. *International Journal of Control* 2002; **75**(6):399–407.
33. Huusom JK, Poulsen NK, Jørgensen SB, Jørgensen JB. ARX-model based model predictive control with offset-free tracking. *Proceeding of 20th European Symposium on Computer Aided Process Engineering*, Ischia, Naples, Italy, June 6–9, 2010; 601–606.
34. Hong X, Mitchell RJ, Chen S, Harris CJ, Li K, Irwin GW. Model selection approaches for non-linear system identification: a review. *International Journal of Systems Science* 2008; **39**(10):925–946.
35. Chen S, Billings SA. Representation of non-linear systems: the NARMAX model. *International Journal of Control* 1989; **49**(3):1013–1032.

DOI: 10.1002/acs

36. Billings SA, Chen S, Korenberg MJ. Identification of MIMO non-linear systems using a forward-regression orthogonal estimator. *International Journal of Control* 1989; **49**(6):2157–2189.
37. Chen S, Billings SA, Luo W. Orthogonal least squares methods and their application to nonlinear system identification. *International Journal of Control* 1989; **50**(5):1873–1896.
38. Chen S, Billings SA, Grant PM. Non-linear systems identification using neural networks. *International Journal of Control* 1990; **51**(6):1191–1214.
39. Vapnik VN. *The Nature of Statistical Learning Theory*. Springer-Verlag: New York, 1995.
40. Narendra KS, Parthasarathy K. Identification and control of dynamical systems using neural networks. *IEEE Transactions on Neural Networks* 1990; **1**(1):4–27.
41. Scokaert POM, Mayne DQ, Rawlings JB. Suboptimal model predictive control (feasibility implies stability). *IEEE Transactions on Automatic Control* 1999; **44**(3):648–654.
42. Chen H, Allgöwer F. A quasi-infinite horizon nonlinear model predictive control scheme with guaranteed stability. *Automatica* 1998; **34**(10):1205–1217.
43. Mayne DQ, Rawlings JB, Rao CV, Scokaert POM. Constrained model predictive control: stability and optimality. *Automatica* 2000; **36**(6):789–814.
44. De Nicolao G, Magni L, Scattolini R. On the robustness of receding-horizon control with terminal constraints. *IEEE Transactions on Automatic Control* 1996; **41**(3):451–453.
45. Scokaert POM, Rawlings JB, Meadows ES. Discrete-time stability with perturbations: application to model predictive control. *Automatica* 1997; **33**(3):463–470.
46. Limón Marreudo D, Álamo T, Camacho EF. Input-to-state stable MPC for constrained discrete-time nonlinear systems with bounded additive uncertainties. *Proceeding of 41st IEEE CDC*, Las Vegas, USA, December 10–13, 2002; 4619–4624.
47. De Nicolao G, Magni L, Scattolini R. Stabilizing predictive control of nonlinear ARX models. *Automatica* 1997; **33**(9):1691–1697.
48. De Nicolao G, Magni L, Scattolini R. Stability and robustness of nonlinear receding horizon control. In *Nonlinear Model Predictive Control*, Vol. 26, Allgöwer F, Zheng A (eds). Birkhauser: Verlag, 2000; 3–22.
49. Imsland L, Findeisen R, Bullinger E, Allgöwer F, Foss BA. A note on stability, robustness and performance of output feedback nonlinear model predictive control. *Journal of Process Control* 2003; **13**(7):633–644.
50. Meadows E, Rawlings J. Model predictive control. In *Nonlinear Process Control*, Henson MA, Seborg DE (eds). Prentice Hall: Upper Saddle River, NJ, 1997; 233–310.
51. Economou CG, Morari M, Palsson BO. Internal model control: extension to nonlinear systems. *Industrial & Engineering Chemistry Process Design and Development* 1986; **25**(2):403–411.
52. Limon D, Alvarado I, Alamo T, Camacho EF. MPC for tracking of piecewise constant references for constrained linear systems. *Automatica* 2008; **44**(9):2382–2387.
53. Ferramosca A, Limon D, Alvarado I, Alamo T, Camacho EF. MPC for tracking with optimal closed-loop performance. *Automatica* 2009; **45**(8):1975–1978.
54. Rodrigues MA, Odloak D. MPC for stable linear systems with model uncertainty. *Automatica* 2003; **39**(4):569–583.
55. Gonzalez AH, Odloak D. Robust model predictive controller with output feedback and target tracking. *IET Control Theory and Applications* 2010; **4**(8):1377–1390.
56. Sistu PB, Bequette BW. Model predictive control of processes with input multiplicities. *Chemical Engineering Science* 1995; **50**(6):921–936.
57. Chang CC, Lin CJ. LIBSVM: a library for support vector machines, September 2001. (Available from: http://www.csie.ntu.edu.tw/~cjlin/libsvm) [Accessed on July 1, 2011].

DOI: 10.1002/acs